

Solar cycle dependence of High-Intensity Long-Duration Continuous AE Activity (HILDCAA) events, relativistic electron predictors?

R. Hajra,¹ E. Echer,¹ B. T. Tsurutani,² and W. D. Gonzalez¹

Received 20 March 2013; revised 31 July 2013; accepted 22 August 2013; published 12 September 2013.

[1] High-Intensity, Long-Duration, Continuous AE Activity (HILDCAA) events are studied using long-term geomagnetic and solar wind/interplanetary databases. We use the strict definition of a HILDCAA event, that it occurs outside of the main phase of a magnetic storm, the peak AE is >1000 nT, and the duration is at least 2 days long. One hundred thirty-three events have been identified from the AE indices in the 1975 to 2011 interval, a $\sim 3\frac{1}{2}$ solar cycle span. Of the 133 events, 99 had simultaneous interplanetary data available. The overwhelming majority (94%) of these latter cases were associated with high-speed solar wind stream (HSS) events. The remaining 6% of the cases occurred after the passage of interplanetary coronal mass ejections (ICMEs). The HSS-related events were typically associated with large interplanetary magnetic field (IMF) Bz variances. The ICME-related events were characterized by steady southward Bz intervals or low-frequency fluctuations, both of which we view as possible different interplanetary phenomena. HILDCAA events have been found to have their largest occurrence frequency in the solar cycle descending phase ($\sim 6.8/\text{year}$) with the second largest at solar minimum ($\sim 3.5/\text{year}$). The occurrence frequencies were considerably lower in the ascending phase ($\sim 2.5/\text{year}$) and at solar maximum ($\sim 2.2/\text{year}$). Thus, HILDCAAs can occur during all phases of the solar cycle, with the descending phase approximately three times more likely to have an event than at solar maximum and the ascending phase. The HILDCAA events that occurred in the declining phase and at solar minimum were $>20\%$ longer in duration than those in the ascending phase and solar maximum, respectively. The events during the recent solar and geomagnetic minima, 2007–2009, were, on the average, $\sim 17\%$ and 14% weaker in peak AE than the events during the previous two minima of 1995–1997 and 1985–1987, respectively. The recent minimum events were $\sim 35\%$ and 41% shorter in durations, respectively, than the events during those previous minima. The yearly occurrence of the events exhibited statistically significant correlation (>0.70) with yearly average speed and number of HSSs. No seasonal dependence of HILDCAA was noted.

Citation: Hajra, R., E. Echer, B. T. Tsurutani, and W. D. Gonzalez (2013), Solar cycle dependence of High-Intensity Long-Duration Continuous AE Activity (HILDCAA) events, relativistic electron predictors?, *J. Geophys. Res. Space Physics*, 118, 5626–5638, doi:10.1002/jgra.50530.

1. Introduction

[2] It has been shown that continuous, intense auroral activity, called High-Intensity, Long-Duration, Continuous AE Activity (HILDCAA) event [Tsurutani and Gonzalez, 1987] is associated with the generation of magnetospheric relativistic electron acceleration [Paulikas and Blake, 1979;

Baker et al., 1986; Summers et al., 1998; Nakamura et al., 2000; Lorentzen et al., 2001; Meredith et al., 2003; Tsurutani et al., 2006a, 2006b]. The scenario posed is that 10–100 keV electrons are injected into the nightside sector of the magnetosphere during impulse substorm and convection events [Horne and Thorne, 1998; Obara et al., 2000; Tsurutani et al., 2006a]. The electrons are heated preferentially in the T_{\perp} direction such that $T_{\perp} > T_{\parallel}$ (T_{\perp} and T_{\parallel} being electron temperatures perpendicular and parallel to the ambient magnetic field, respectively) through the injection process and thus are unstable to the temperature anisotropy instability [Kennel and Petschek, 1966; Tsurutani et al., 1979; Tsurutani and Lakhina, 1997] generating electromagnetic plasma waves called chorus [Gurnett and O'Brien, 1964; Burtis and Helliwell, 1969; Tsurutani and Smith, 1974, 1977; Meredith et al., 2003; Tsurutani et al., 2011a]. Cyclotron resonance between the plasma waves and the

¹Instituto Nacional de Pesquisas Espaciais (INPE), São José dos Campos, São Paulo, Brazil.

²Jet Propulsion Laboratory (JPL), California Institute of Technology, Pasadena, California, USA.

Corresponding author: R. Hajra, Instituto Nacional de Pesquisas Espaciais (INPE), Av. dos Astronautas, 1758, São José dos Campos, SP, 12227-010, Brazil. (raj.kumarhajra@yahoo.co.in)

©2013. American Geophysical Union. All Rights Reserved.
2169-9380/13/10.1002/jgra.50530

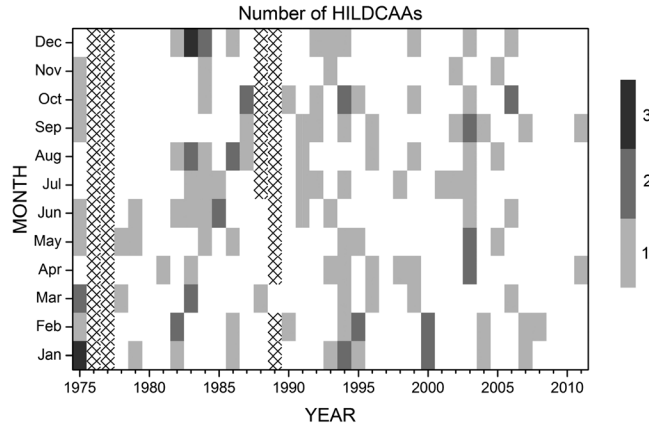


Figure 1. The number of HILDCAAs for different months of the years 1975–2011. The values of different shadings are given in the legend at the right. The crosses represent data gaps from January 1976 to December 1977, from July 1988 to February 1989, and from April to December of 1989.

electrons leads to pitch angle scattering of the electrons and loss to the ionosphere [Inan *et al.*, 1978; Thorne *et al.*, 2005; Summers *et al.*, 2007; Tsurutani *et al.*, 2009, 2013; Lakhina *et al.*, 2010]. The waves also interact with the electrons by phase-trapping them [Li *et al.*, 1997; Omura *et al.*, 2008], leading to the acceleration of electrons to relativistic energies. It is generally accepted that these continuous, intense auroral activity events are associated with high-speed solar wind streams (HSSs) which emanate from coronal holes [Sheeley *et al.*, 1976; Tsurutani and Gonzalez, 1987; Tsurutani *et al.*, 1995].

[3] The purpose of this effort is to study HILDCAA events from 1975 to 2011 to determine the solar cycle and seasonal dependences of this phenomenon for the first time. The properties of these events such as the temporal length, and the peak, average and integrated intensities will be characterized. The results of this survey and a list of the events will be available, upon request, for studies of chorus, relativistic electrons, as well as ionospheric and geomagnetic effects.

2. Data Used and Method of Analyses

2.1. HILDCAA Criteria

[4] In the present study, all HILDCAA events occurring during 1975–2011 were identified when data were available. The events were selected using the following four criteria of Tsurutani and Gonzalez [1987]:

- [5] 1. the events had peak AE intensities greater than 1000 nT,
- [6] 2. the events had durations at least 2 days in length,
- [7] 3. the high AE activity was continuous throughout the interval, i.e., AE never dropped below 200 nT for more than 2 h at a time, and
- [8] 4. the events occurred outside the main phases of geomagnetic storms.

[9] It should be mentioned that the “HILDCAA criteria” originally selected by Tsurutani and Gonzalez [1987] were stringent in order to minimize the number of events to be studied. The same physical process may occur when one or more of the four criteria are not strictly followed. It was also stressed that the mechanisms creating HILDCAAs must be separate from those creating magnetic storm

main phases. It should also be noted that the acronym HILDCAA contains the term “AE activity” and does not indicate only substorm activity [see Tsurutani *et al.*, 2004 and Guarnieri, 2006].

2.2. Geomagnetic and Interplanetary Data

[10] To identify HILDCAA events, 1 min AE indices from the World Data Center for Geomagnetism, Kyoto, Japan (<http://wdc.kugi.kyoto-u.ac.jp/>) were used. The Dst indices (1 h time resolution) used to identify geomagnetic storm main phases were obtained from Echer *et al.* [2011a]. Our definition of a magnetic storm main phase was an interval of a decrease in Dst with peak $Dst < -50$ nT [Akasofu, 1981; Gonzalez *et al.*, 1994]. Descriptions of the indices may be found in Sugiura [1964], Davis and Sugiura [1966], and Rostoker [1972]. To identify HILDCAA intervals, $AE > 1000$ nT events were first sought. The data were scanned both forward and backward in time to determine where the event decreased below 200 nT for 2 h or more. If this event was outside of a storm main phase and the event was longer than 2 days, this was categorized as a HILDCAA event.

[11] One hundred thirty-three events were identified during the study interval. In Figure 1, the distribution of the HILDCAA events is shown as a function of both year and month. The crosses in the figure indicate data gaps.

[12] Solar wind/interplanetary data at 1 min time resolution were obtained from the OMNI website (<http://omniweb.gsfc.nasa.gov/>). OMNI interplanetary data had been already time adjusted to take into account the solar wind convection time from the spacecraft to the bow shock, so no further adjustments to the interplanetary data used were made in this study (see http://omniweb.gsfc.nasa.gov/html/omni_min_data.html).

2.3. Solar Cycle and Seasonal Dependences

[13] To study the HILDCAA event solar cycle dependence, the events were first separated into individual solar cycles (SCs). They are: SC 21 (1975–1985), SC 22 (1986–1995), SC 23 (1996–2005), and SC 24 (2006–2011). The solar cycles were then divided into four phases, the ascending phase (1977–1978, 1987–1988, 1998–1999, 2011), solar maximum (1979–1981, 1989–1991, 2000–2002), the descending phase (1982–1984, 1992–1994, 2003–2005), and solar minimum

7-16 December 2003

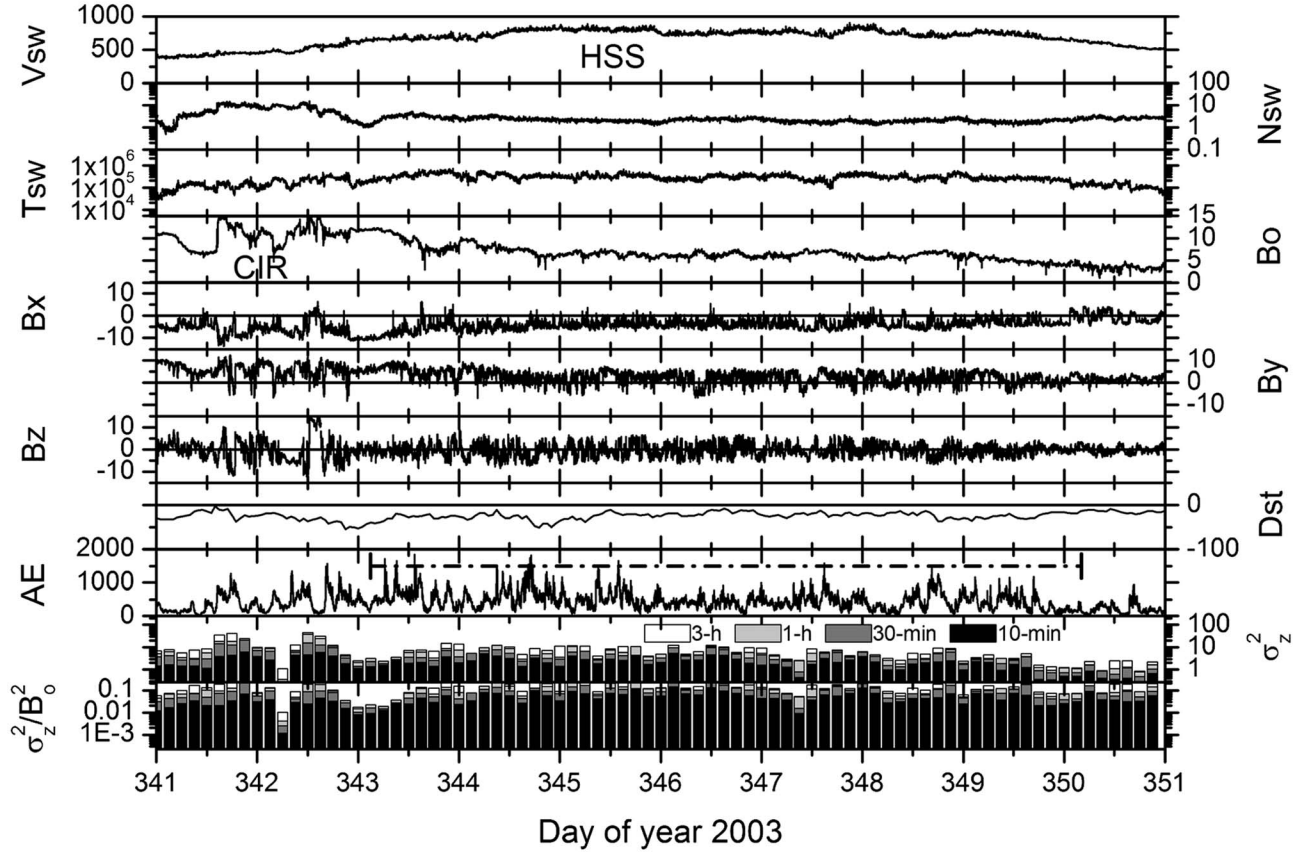


Figure 2. Solar wind/interplanetary parameters and geomagnetic activity indices for a HILDCAA event during December 2003. From top to bottom, the panels show the variations of solar wind speed (V_{sw} in km/s), plasma density (N_{sw} in cm^{-3}), temperature (T_{sw} in K), IMF magnitude (B_0 in nT), and B_x (nT), B_y (nT), B_z (nT) components in the GSM coordinate system, and the Dst (nT), AE (nT) indices, respectively. The bottom two panels show the nested 10 min, 30 min, 1 h, and 3 h variances (σ_z^2 in nT^2) and normalized variances (σ_z^2/B_0^2) of B_z . The legend for the variances and normalized variances is given in the next to last panel. The variances are estimated using 1 min IMF data. In the AE panel, the horizontal dash-dotted line indicates the time interval of the HILDCAA event. There are high amplitude Alfvén waves in IMF B_z during the HILDCAA interval. This event was caused by the southward components of the IMF Alfvén waves in a CIR/HSS.

(1975–1976, 1985–1986, 1995–1997, 2006–2010). The events were also divided into seasons of the year. The seasons are defined as follows: northern hemisphere spring equinox (February, March, April), summer solstice (May, June, July), fall equinox (August, September, October), and winter solstice (November, December, January).

[14] Annual averaged $F_{10.7}$ solar flux ($10^{-22} \text{Wm}^{-2} \text{Hz}^{-1}$) data (<http://www.drao.nrc.ca/icarus>) were used to identify solar cycle phases. Although there is little difference in the solar cycle phases between those shown in $F_{10.7}$ and sunspot numbers, it was felt that $F_{10.7}$ was more appropriate [Doherty *et al.*, 2000] for a study that involved HSSs emanating from coronal holes.

2.4. Nested and Normalized Variances

[15] Nested variances of the interplanetary magnetic field (IMF) components [Tsurutani *et al.*, 1982] were calculated to have a quantitative measure of interplanetary Alfvén wave intensities [Tsurutani *et al.*, 2011a, 2011b; Echer *et al.*,

2011b]. Since interplanetary Alfvén wave fluctuations are more or less isotropic and B_z is an important component leading to geomagnetic activity at Earth [Dungey, 1961], only the B_z component variances (σ_z^2) are shown in the paper. The 10 min, 30 min, 1 h, and 3 h variances were calculated from 1 min average magnetic field data and then were used to make 3 h averages of those quantities. Because the 3 h values are greater than the 1 h values, 1 h values are greater than the 30 min values (for the same time interval), and so on, the lowest time scale variance is “nested” inside the value of the next higher time scale variance, etc. The scientific benefit of this method of data display is that the variances give the amount of wave power for frequencies up to the variance value. For example, the 3 h average 30 min variance values represent the average wave power occurring in the 1 min (the highest resolution of the data used) to 30 min wave period range. The 1 h variance values give the wave power occurring between 1 min and 1 h wave power range. If one subtracts the 30 min variance value from the 1 h variance

14-18 May 2005

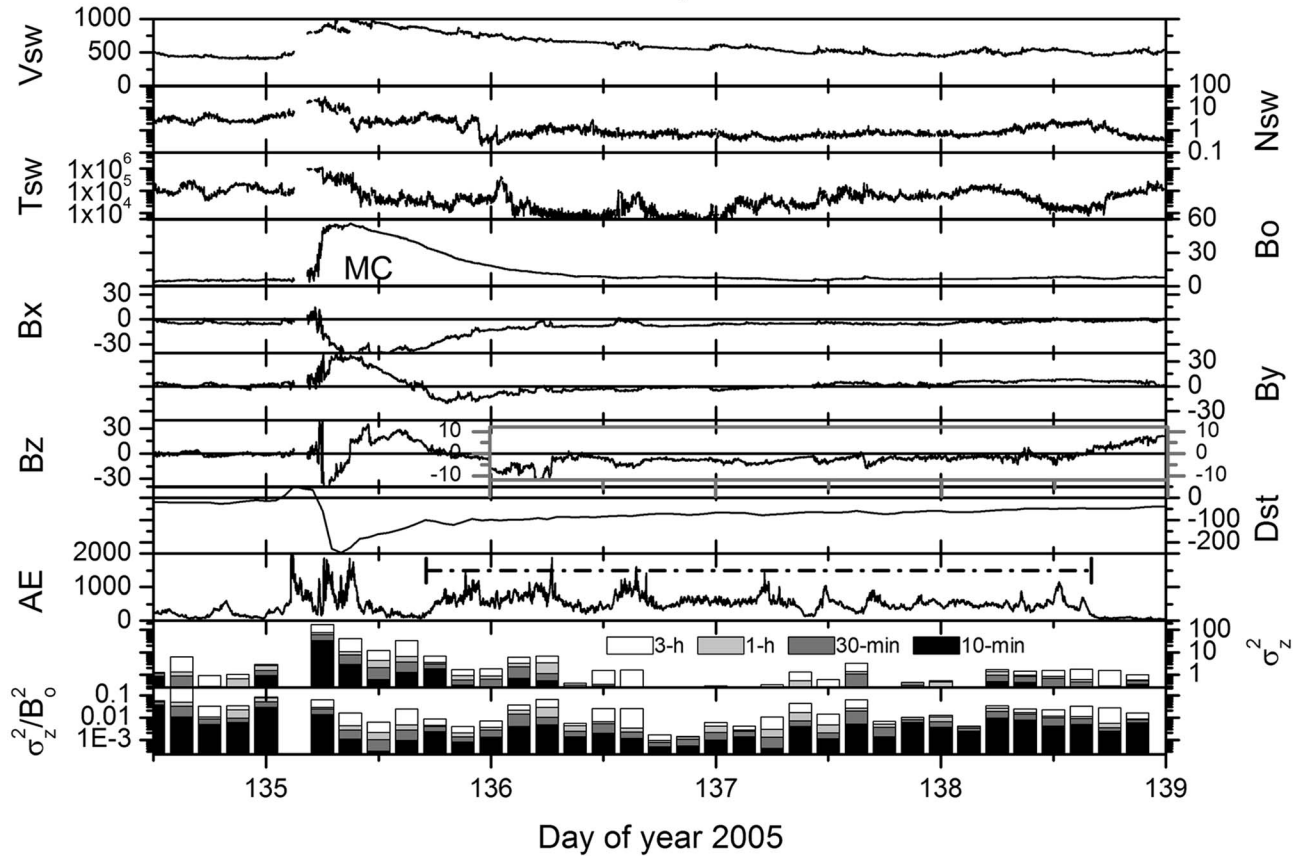


Figure 3. Another example of HILDCAA event but associated with an ICME. The event occurred during May 2005. The format is the same as in Figure 2. This HILDCAA follows a magnetic cloud (MC). Note that the IMF B_z during the HILDCAA-interval (marked by box in B_z panel) are shown in enhanced scale to make clear viewing. The IMF B_z value is slightly negative throughout the entire HILDCAA interval. It is generally devoid of Alfvén waves, unlike the case shown in Figure 2.

value, the resultant value is the amount of wave power which was present for wave periods between 30 min and 1 h. Variances are also easy to calculate and display. They can be used to determine an average wave power and a low-resolution power spectrum.

[16] The variance values were also normalized by dividing the variance values by the square of the magnetic field magnitude (B_o^2). We call these the “normalized variances,” σ_z^2/B_o^2 . This quantity is the most important quantity for cyclotron resonant wave-particle interactions [Kennel and Petschek, 1966; Tsurutani and Lakhina, 1997].

3. Results

[17] Figure 1 shows all of the HILDCAA intervals detected during the interval of study. From the figure, it is seen that HILDCAAs may occur during any month and during any year. There are only a few regions where there are many events. Three intervals stand out from the rest: (i) May–August 1983–1985, (ii) January–May 1993–1995, and (iii) April–October 2002–2003. All three of these intervals are in the declining phases of the solar cycle (more will be stated about this later). However, the seasons are quite different. The first interval is during summer, the second during spring, and the third during summer-fall.

3.1. Case Studies on HILDCAA Events

[18] An example of a HILDCAA event and associated solar/interplanetary variations during December 2003 is shown in Figure 2. As denoted by the horizontal dash-dot line in the AE panel, the event started at ~0248 UT on day 343 (9 December), 2003 and continued for ~7 days until ~0402 UT on day 350 (16 December). The peak intensity (AE) of the event was ~1840 nT. This HILDCAA event was preceded by the main phase of a moderate intensity geomagnetic storm ($Dst = -54$ nT). The inspection of the solar wind and interplanetary data indicates that the event occurred during an HSS-interval. The HSS had a peak solar wind speed (V_{sw}) of ~860 km/s. It started by the middle of day 342 and persisted until day 350. The solar wind temperature (T_{sw}) more-or-less followed the variation of V_{sw} [Lopez and Freeman, 1986].

[19] Compressions in plasma and magnetic fields at the interface between the HSS and the slow stream in the antisolar direction (upstream) of the HSS are evident in the increases of plasma density (N_{sw}) and IMF magnitude (B_o). This can be noted from ~0309 UT on day 341 to 1522 UT on day 343. These signatures identify this as a corotating interaction region (CIR) [Smith and Wolfe, 1976; Tsurutani et al., 2006a]. For more details of HSS-slow-speed stream

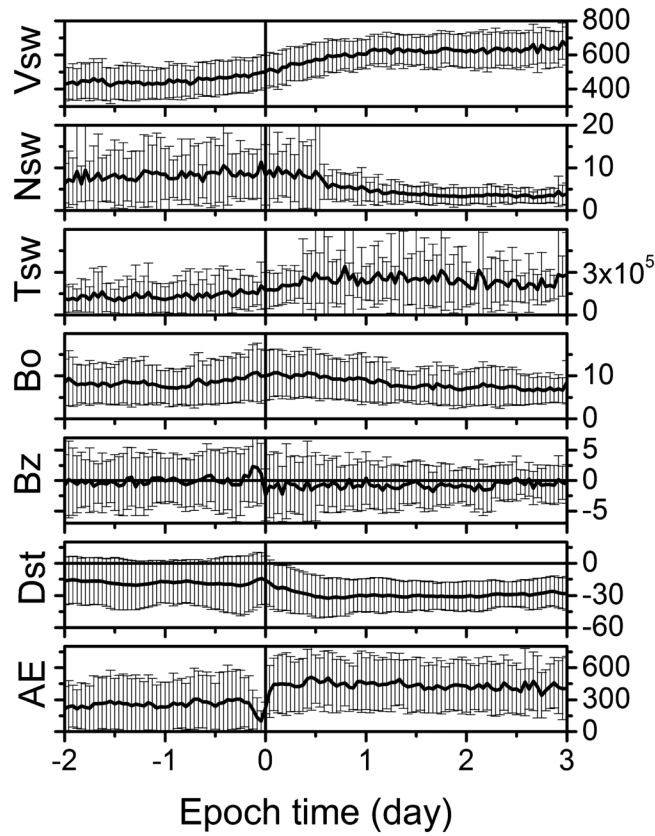


Figure 4. Superposed epoch analyses results for 93 HILDCAA events associated with HSS/CIR events showing, from top to bottom panels, Vsw (km/s), Nsw (cm^{-3}), Tsw (K), IMF Bo (nT), Bz (nT), Dst (nT), and AE (nT). The solid lines are the mean values and vertical bars represent the standard deviations. The zero epoch time corresponds to the starting time of the events.

interactions, we refer the reader to *Hundhausen* [1973] and *Pizzo* [1985].

[20] During the HILDCAA interval, Bz had an average value of ~ -0.41 nT. In the next to lowermost panel, 3 h averages of 10 min, 30 min, 1 h, and 3 h nested variances of Bz are displayed. The bottom panel gives the normalized variances of Bz. As can be observed from the figure, the variance values were enhanced (3 h variance ~ 47 nT^2 , 1 h ~ 39 nT^2) near the stream-stream interaction region where the magnetic field was strongly compressed. This result is similar to results of analysis of other HSSs, one occurring in 2003 [*Tsurutani et al.*, 2011a] and another in 2008 [*Echer et al.*, 2011b]. During the HSS-interval, the 3 h (1 h) variance ranged from ~ 1.17 to 15 nT^2 (~ 0.92 – 12 nT^2), with the average value ~ 7 nT^2 (5 nT^2). The normalized variances were found to be comparable during the stream interaction region and HSS-interval. The peak, minimum, and average values of 3 h (1 h) normalized variances were $\sim 3.4 \times 10^{-1}$, 1.8×10^{-2} , and 1.5×10^{-1} (0.3×10^{-1} , 1.8×10^{-2} , and 1.2×10^{-1}), respectively.

[21] Figure 3 shows another example of a HILDCAA event during May 2005. The Dst intensity indicates the presence of an intense geomagnetic storm (Dst = -263 nT) during the first half of day 135 (15 May), 2005. The recovery phase started at ~ 0900 UT on this day. The intense storm was caused by the southward IMF Bz of the magnetic cloud (MC)/interplanetary coronal mass ejection (ICME) [*Klein and Burlaga*, 1982; *Tsurutani et al.*, 1988; *Echer et al.*,

2008]. The IMF Bz was intensely southward (~ -45 nT) for more than 3 h. The situation was favorable for the development of the superintense storm main phase [*Tsurutani et al.*, 1992; *Echer et al.*, 2008]. A peak solar wind speed (Vsw) of ~ 980 km/s was detected during the main phase of the storm. The variation of the AE index during the storm recovery phase indicates the presence of a HILDCAA from ~ 1708 UT on day 135 (15 May) to ~ 1603 UT on day 138 (18 May). The peak (AE) intensity was ~ 1870 nT.

[22] The IMF Bz variation during the HILDCAA interval (marked by box) is shown amplified for better viewing. Bz exhibited a small, continuous southward component (average ~ -2.8 nT). The low-frequency southward component is associated with the HILDCAA. The two lowermost panels show the nested and normalized variances of Bz for the whole interval. The variances were intense during the storm main phase (peak 3 h variance ~ 174 nT^2 , 1 h ~ 78 nT^2). During the HILDCAA-interval, the 3 h (1 h) variance varied from ~ 0.09 to 6.81 nT^2 (~ 0.07 – 3.56 nT^2), with an average value of ~ 1.71 nT^2 (0.87 nT^2). The peak, minimum, and average values of 3 h (1 h) normalized variances were 6.3×10^{-2} , 1.4×10^{-3} , and 1.9×10^{-2} (2.9×10^{-2} , 0.96×10^{-3} , and 0.96×10^{-2}), respectively. These variance and normalized variance values were considerably smaller than those for event 1 (Figure 2).

[23] From the case studies, we found that while the HSS-related event (Figure 2) was associated with large-amplitude Bz variances, the ICME-related event (Figure 3) was characterized by small, steady southward IMF Bz intervals or

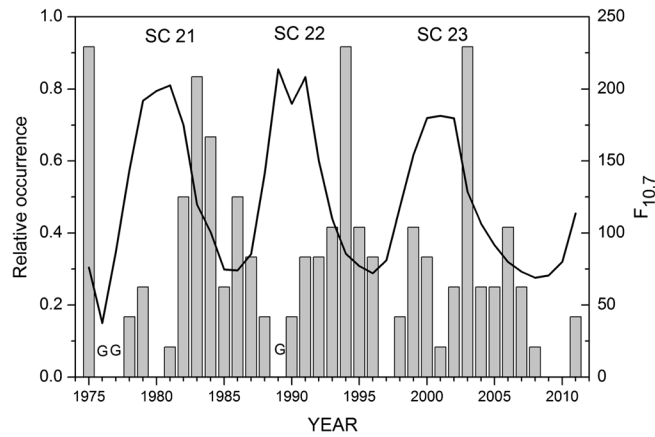


Figure 5. Histograms give the relative occurrence of HILDCAAs during different years of observations (1975–2011) (see text for details). The continuous line (secondary y axis, legend on the right) shows the yearly smoothed $F_{10.7}$ solar flux. “G” represents data gap. No AE data were available for the years 1976 and 1977. For the year 1988, AE data were only available from January to June, and for the year 1989, AE data were available only for the month of March.

low-frequency fluctuations. We view this as a possible different interplanetary mechanism for the geomagnetic activity/HILDCAA. There were 99 HILDCAA events where interplanetary data were available. It was found that 93 of the events (94%) were associated with CIRs/HSSs. Only six events occurred after the passage of ICMEs. The peak 3 h variance for the 93 CIR-events ranged from ~ 5.1 to 130 nT^2 , with an average value of 34 nT^2 . On the other hand, the peak 3 h variance for the six ICME-related events varied between ~ 2.41 and 45.4 nT^2 , with average value of 15.3 nT^2 . Thus, the IMF B_z variances for the CIR-related events were larger than those for the ICME-events. We note, however, a lack of a significantly large database to draw statistical conclusions.

3.2. Superposed Epoch Analyses

[24] Superposed epoch analyses were performed on the geomagnetic and solar/interplanetary variations for the 93 events associated with HSS/CIR events. The initiation times of HILDCAA events were taken as the zero epoch time. Figure 4 depicts the superposed mean variations and standard deviations of V_{sw} , N_{sw} , T_{sw} , IMF B_o , B_z , Dst , and AE indices. The variations of the parameters from 2 days prior to 3 days after the start time of HILDCAAs are shown. The superposed variations may give some qualitative idea about the general features of geomagnetic activity and causative interplanetary variations during HILDCAA events.

[25] The variations of solar/interplanetary data show typical interplanetary signatures of CIRs (as was illustrated for event 1, Figure 2). The interaction between an HSS and an upstream (antisunwardly located) slow-speed stream is evident in the increase ($\sim 48\%$) of average V_{sw} around zero epoch time. An increase of $\sim 118\%$ was noted in T_{sw} around the stream interface location. A compression in plasma and magnetic field was evident in the increases of N_{sw} ($\sim 38\%$) and of B_o ($\sim 42\%$) from ~ 14 h prior to 18 h after the zero epoch time. The enhanced T_{sw} and B_o on the right side of the zero epoch time represent the compressed fast stream. On the left side of the zero epoch time, there is a mixture of two effects affecting the plasma and fields. There is a

compression of the slow solar wind leading to higher plasma densities, temperatures, and magnetic fields. There are also naturally occurring high plasma densities near the heliospheric current sheet (HCS) [Smith *et al.*, 1978; Tsurutani *et al.*, 1995], called the heliospheric plasma sheet (HPS: Winterhalter *et al.* [1994]). A superposed epoch analysis of this type mixes these different physical phenomena.

[26] Some noteworthy features in Figure 4 are: (i) before event initiation, the average B_z value was $\sim 0 \text{ nT}$; (ii) B_z showed northward-to-southward turning ~ 2.5 h prior to the event initiation; and (iii) B_z remained negative, though with very small peak value ($\sim -2.4 \text{ nT}$), during the event interval. The northward-to-southward turning may represent the typical HCS crossing or sector reversal of the IMF occurring prior to stream interaction [Smith *et al.*, 1978]. The $B_z \sim 0 \text{ nT}$ prior to zero epoch was related to the “magnetic calm” [Tsurutani *et al.*, 1995, 2006a, 2006b; Borovsky and Steinberg, 2006] as evident in low values of Dst ($> -20 \text{ nT}$) and AE ($\sim 300 \text{ nT}$). Although we observed high-frequency fluctuations between northward and southward directions in B_z during individual HILDCAA events (see Figure 2), the superposed variation (average) showed only nearly constant southward values. This result is related to the averaging process of large fluctuations over many events. This superposed southward component of B_z after the sector reversal facilitated the magnetospheric reconnection mechanism [Dungey, 1961; Gonzalez and Mozer, 1974] and is consistent with weak but sustained geomagnetic activity observed in the AE (average value $\sim 450\text{--}500 \text{ nT}$) and Dst ($< -30 \text{ nT}$) variations.

[27] In the following sections, results of the statistical study on the solar cycle and seasonal dependences as well as the geomagnetic characteristics of HILDCAAs are presented.

3.3. Solar Cycle Dependences of HILDCAAs

[28] We investigate the solar cycle dependence of 133 HILDCAA events by first identifying the months and years of occurrences. The number of events during each year was divided by the number of months of observation in that

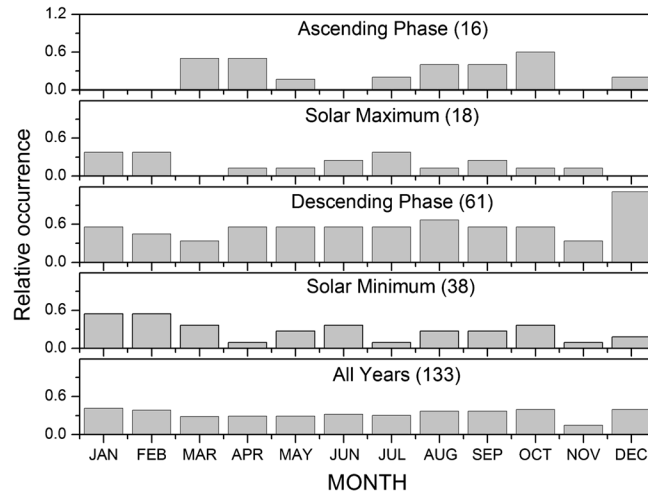


Figure 6. Histograms show the relative occurrence of HILDCAAs during each month. From top to bottom, the panels show the results during the ascending phase, solar maximum, the descending phase, solar minimum, and during the entire period of observation, respectively. The numbers in the parentheses represent the total number of events during each interval.

year (Figure 5). This process corrects the distribution for data gaps. HILDCAA events were found to be distributed primarily around the declining phase and solar minimum. The highest peak occurrences were noted during the

declining phase of the solar cycle. Averaging over the solar cycles, it was observed that the occurrence rate of events during the declining phase was $\sim 6.8/\text{year}$. The next most frequent event occurrence happened at solar minimum

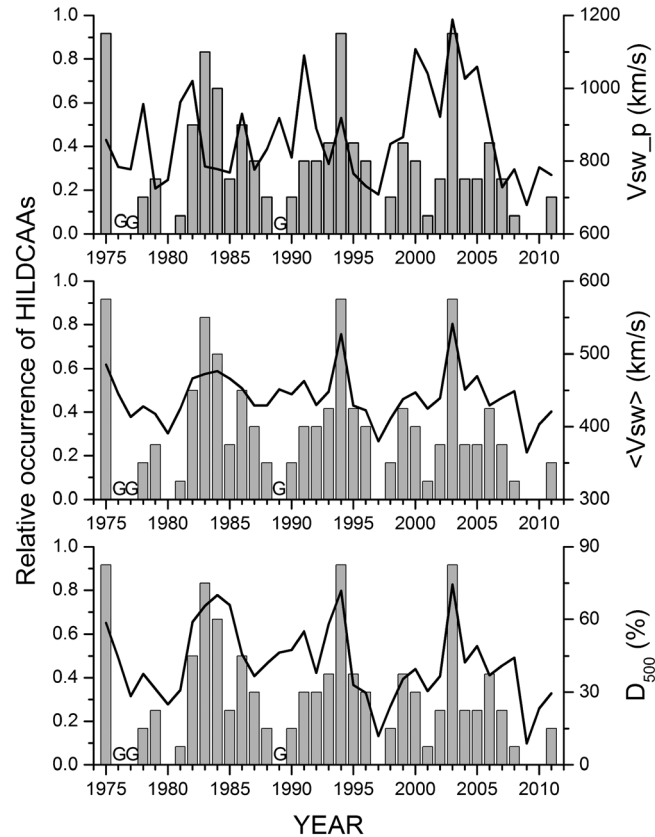


Figure 7. Histograms showing the relative occurrence of HILDCAAs during different years of observation (1975–2011). The continuous lines (secondary y axis, legend on the right) present the yearly peak (V_{sw_p}) and yearly average ($\langle V_{sw} \rangle$) of solar wind speed and the percentage of days (D_{500}) with $V_{sw} \geq 500$ km/s. “G” represents data gap.

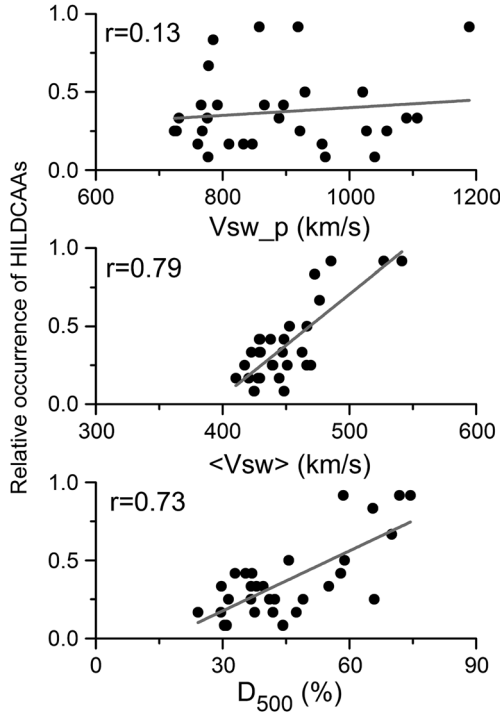


Figure 8. The scatter plots showing the relative occurrences of HILDCAAs during each year versus V_{sw_p} , $\langle V_{sw} \rangle$, and D_{500} . The linear regression curves and the corresponding correlation coefficients (r) are also given.

(~ 3.5 /year). HILDCAA events also occurred at solar maximum (~ 2.2 /year) and in the ascending phase (~ 2.5 /year). Thus, HILDCAAs occurred in all phases of the solar cycle. During the declining phase, the occurrence rate was approximately three times as likely as during solar maximum and in the ascending phase.

[29] Interesting differences between the solar cycles were noted. Around the transition between the SCs 21 and 22, a two-peak nature of HILDCAA occurrence was evident. However, only one peak was noted for the SCs 22–23 transition. Although, two peaks were observed in the descending phase of SC 23, the events were found to be more evenly distributed throughout this cycle.

[30] The solar cycle dependence of HILDCAAs depicted here is different from the reported solar cycle dependence of intense ($Dst < -100$ nT) geomagnetic storms [Gonzalez *et al.*, 1990, 1994, 2007; Alves *et al.*, 2006; Tsurutani *et al.*, 2006a; Echer *et al.*, 2008, 2011a, 2013; Chakraborty and Hajra, 2010; Hajra, 2011]. The largest occurrence of the storms is at and around solar maximum. The minimum occurrence of storms is at solar cycle minimum phase.

[31] At solar maximum and a few years after solar maximum, the main features present at the Sun are sunspots and active regions. Intense solar flares and coronal mass ejections (CMEs) [Burlaga *et al.*, 1981; Klein and Burlaga, 1982; Gosling *et al.*, 1990] often occur together because they are both products of solar magnetic reconnection. If these ICMEs have southward B_z components and they hit the Earth's magnetosphere, they cause magnetic storms. At solar maximum, ICMEs are known to be the main causes of geomagnetic storms [Tsurutani *et al.*, 1988; Gosling *et al.*, 1990; Richardson *et al.*, 2002; Echer *et al.*, 2008]. The yearly number of CMEs, yearly

peak, and average CME speeds are reported to exhibit an ~ 11 year solar cycle variation [Webb and Howard, 1994; Gopalswamy *et al.*, 2004; Obridko *et al.*, 2012] similar to that of intense geomagnetic storms [Tsurutani *et al.*, 2006a].

[32] During the declining phase and solar minimum, coronal holes extend to lower solar latitudes and expand in size, becoming the dominant solar feature causing geomagnetic activity. HSSs emanate from these coronal holes [Krieger *et al.*, 1973; Sheeley *et al.*, 1976; Tsurutani *et al.*, 1995]. CIRs are formed at the leading edges of the fast streams due to interaction with slow background streams [Smith and Wolfe, 1976; Pizzo, 1985; Balogh *et al.*, 1999]. CIRs usually lead to moderate magnetic storms ($Dst > -100$ nT: Tsurutani and Gonzalez [1997]) and the trailing HSS proper causes prolonged periods of geomagnetic activity [Tsurutani *et al.*, 1995; Guarnieri *et al.*, 2006; Kozyra *et al.*, 2006; Turner *et al.*, 2006]. The HSS/HILDCAA intervals appear as a “recovery phase” of the CIR storm, but in actuality there is fresh input of solar wind energy in addition to the ring current decay [Tsurutani *et al.*, 2004; Guarnieri, 2006]. Thus, the HILDCAA solar cycle distribution follows the low-latitude coronal hole distribution at the Sun and the CIR/HSS distribution in the solar wind in the ecliptic plane.

3.4. Seasonal Dependences of HILDCAAs

[33] To study the seasonal dependences, the number of events in a month was divided by the number of years where

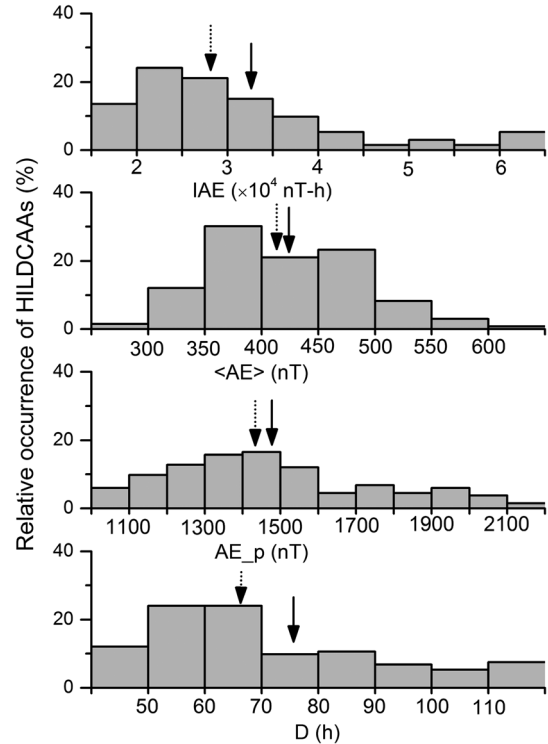


Figure 9. Histograms of HILDCAAs for different ranges of (a) IAE (10^4 nT-h), (b) $\langle AE \rangle$ (nT), (c) AE_p (nT), and (d) D (h). These histograms are for the 133 events occurring during entire period of observation (1975–2011). The downward arrows in each panel indicate the corresponding average (solid) and median (dotted) values. The lower limits of the parameters are: $D > 48$ h, $AE_p > 1000$ nT, and $\langle AE \rangle > 200$ nT. These were by definition.

Table 1. Statistical Features of 133 HILDCAA Events Occurring During 1975–2011

	Average \pm SD	Median	Maximum	Minimum
IAE (10^4 nT-h)	3.3 ± 2	2.8	16.3	1.4
$\langle \text{AE} \rangle$ (nT)	422 ± 67.5	418.5	620.5	284.5
AE _p (nT)	1477.9 ± 277.6	1425	2155	1041
D (day)	3.2 ± 1.5	2.8	12.4	2

observations were available for that particular month. Figure 6 shows the HILDCAA distributions during different months of varying solar cycle phases. From the distribution, it is noted that HILDCAAs exhibited no “classical” semiannual seasonal distribution like that for geomagnetic storms [Chua de Gonzalez et al., 1993; Gonzalez et al., 1999; Echer et al., 2011a]. There were, however, minor seasonal features, which we mention below. There were lesser occurrences during the month of November. This feature was present for all phases of the solar cycle. During solar maxima and the descending phases, the occurrence rate of solstice events appeared to increase slightly. An overall increase in the number of events during the descending phases compared to those during the ascending phases was prominent. Even and odd solar cycle data were grouped together to maintain consistent solar magnetic field polarities (not shown). No clear semiannual or seasonal dependences were noted. The results are in agreement with the Mursula et al. [2011] conclusion, although using a different approach, of ionospheric conductivity control on geomagnetic activity.

3.5. Association of HILDCAAs With HSSs

[34] Figures 7–8 show the HILDCAA event relationship with HSS properties. In Figure 7, the yearly peak (V_{sw_p}) and average ($\langle V_{sw} \rangle$) values of solar wind speed (V_{sw}), and the percentage of days (D_{500}) with HSSs ($V_{sw} \geq 500$ km/s) are compared with yearly occurrences of HILDCAAs (number per month in each year). The peaks in $\langle V_{sw} \rangle$ and D_{500} coincided strongly with the yearly peak occurrences of HILDCAAs, while HILDCAAs did not follow the variation of V_{sw_p} .

[35] Figure 8 shows the variations of yearly occurrences of HILDCAAs with yearly values of V_{sw_p} , $\langle V_{sw} \rangle$, and D_{500} . HILDCAA occurrence was strongly correlated to $\langle V_{sw} \rangle$ and D_{500} and had its poorest correlation with V_{sw_p} . Based on the analysis, we obtained the following relations for HILDCAA occurrence rate:

$$H = (-2.6 \pm 0.4) + (65.5 \pm 9.4) \times 10^{-4} \langle V_{sw} \rangle \quad (r = 0.79) \quad (1)$$

$$H = (-0.2 \pm 0.1) + (1.3 \pm 0.2) \times 10^{-2} D_{500} \quad (r = 0.73) \quad (2)$$

[36] Here H represents the number of HILDCAAs per month in each year. The relationships are statistically significant with high correlation coefficients (r). r is 0.79 in equation 1 (correlation with V_{sw}) and 0.73 in equation 2 (with D_{500}).

[37] Higher values of $\langle V_{sw} \rangle$ and D_{500} may indicate yearly dominance of long-lasting corotating HSSs. The HSSs are accompanied by large-amplitude, nonlinear, long-duration Alfvén wave trains [Belcher and Davis, 1971; Tsurutani et al., 2005, 2006a, 2006b]. A particular good example of this is the HSSs that occurred in 1973–1975 [Tsurutani et al., 1995]. It should be mentioned that such

strong HSS activity that occurred in 1973–1975 has never happened again. The magnetospheric reconnection between southward components of Alfvénic IMF and the Earth’s magnetic field causes continuous energy injection leading to long-sustained high-intensity auroral activities or HILDCAAs [Tsurutani and Gonzalez, 1987; Tsurutani et al., 1990, 1995; Gonzalez et al., 2006].

3.6. Characteristics of HILDCAAs

[38] We identified different characteristics of each HILDCAA event: (i) the time-integrated AE value throughout the event (IAE), (ii) the average AE value during the event ($\langle \text{AE} \rangle$), (iii) the peak AE value for the event (AE_p), and (iv) the duration of the event (D). Figure 9 shows the relative distributions (histograms) of the events with respect to the characteristic parameters for the entire years of study (1975–2011). The results are summarized in Table 1. IAE varied between 1.4×10^4 and 16×10^4 nT-h with an average value of 3.3×10^4 nT-h. About 50% of the events exhibited IAE values in the range of $2\text{--}3 \times 10^4$ nT-h and the number of events decreased gradually for larger values of IAE. The $\langle \text{AE} \rangle$ for the events varied in the range of 285–621 nT, with an average value of 422 nT. The majority of the events were characterized by $\langle \text{AE} \rangle \sim 350\text{--}500$ nT. The HILDCAAs exhibited peak strengths (AE_p) varying from 1041 to 2155 nT with an average value of 1478 nT. More than 50% of the events had an AE_p in the range of 1200–1600 nT. The duration (D) of HILDCAAs was found to vary from a minimum of ~ 2 days (by definition) to more than 12 days (297 h). The average duration was 3.2 days (~ 76 h). The majority of the events ($\sim 60\%$) had 2 to 3 days (50–70 h) durations.

3.7. Solar Cycle Phase Dependences of HILDCAA Characteristics

[39] The HILDCAA events were separated according to their occurrences during different phases of the solar cycle. The solar cycle phase dependences of the HILDCAA

Table 2. Statistical Features of HILDCAAs During Different Solar Activity Conditions^a

	Average \pm SD	Median	Maximum	Minimum
Solar Minimum (38)				
IAE (10^4 nT-h)	3.5 ± 2.7	2.9	16.3	1.6
$\langle \text{AE} \rangle$ (nT)	409.8 ± 59.7	396.1	549.1	302.4
AE _p (nT)	1550.2 ± 290.5	1494	2155	1041
D (day)	3.5 ± 2	2.8	12.4	2
Solar Maximum (18)				
IAE (10^4 nT-h)	2.8 ± 1.1	2.4	5.4	1.7
$\langle \text{AE} \rangle$ (nT)	428.6 ± 73.9	418.3	579.2	327
AE _p (nT)	1351.2 ± 224.5	1307.5	1866	1042
D (day)	2.7 ± 0.8	2.5	5.3	2
Ascending Phase (16)				
IAE (10^4 nT-h)	2.8 ± 0.8	2.7	4.5	1.6
$\langle \text{AE} \rangle$ (nT)	422.1 ± 60.5	419.5	533.2	302.4
AE _p (nT)	1464.6 ± 254.2	1415.5	2155	1058
D (day)	2.7 ± 0.7	2.6	4.4	2
Descending Phase (61)				
IAE (10^4 nT-h)	3.5 ± 2.3	2.8	16.3	1.4
$\langle \text{AE} \rangle$ (nT)	422.8 ± 71	418.5	620.5	284.5
AE _p (nT)	1493.7 ± 280.6	1458	2088	1041
D (day)	3.3 ± 1.7	2.8	12.4	2

^aNumbers of events under each group are also shown.

Table 3. Statistical Features of HILDCAAs Around Three Consecutive Solar Minima^a

	Average \pm SD	Median	Maximum	Minimum
1985–1987 (13)				
IAE (10^4 nT-h)	2.9 ± 0.8	2.9	4	1.6
<AE> (nT)	395.6 ± 50.3	391.8	478.6	327.8
AE _p (nT)	1537.1 ± 335.2	1506	2155	1041
D (day)	3.1 ± 0.7	3	4.3	2.1
1995–1997 (9)				
IAE (10^4 nT-h)	2.9 ± 1.1	2.6	5.5	1.8
<AE> (nT)	409 ± 62.9	416.4	486.4	302.4
AE _p (nT)	1573.7 ± 198	1512	2015	1352
D (day)	2.9 ± 0.9	2.8	5	2.2
2007–2009 (4)				
IAE (10^4 nT-h)	1.9 ± 0.4	1.8	2.4	1.6
<AE> (nT)	364.9 ± 32.6	371.2	392.1	325
AE _p (nT)	1347.3 ± 203.9	1418.5	1494	1058
D (day)	2.2 ± 0.3	2.1	2.6	2

^aNumbers of events under each group are also shown.

characteristics are summarized in Table 2. The events occurring during solar minimum were, on the average, $\sim 29\%$ longer than those during solar maximum. Similarly, the events occurring during the descending phase were $\sim 21\%$ longer than those during the ascending phase.

[40] During the descending and solar minimum phases, HILDCAAs exhibited appreciably larger ranges as well as average values of IAE, AE_p, and D than during the ascending phase and solar maximum, respectively. On the other hand, the <AE> for the events during solar maximum was found to be comparable or even little larger than that during solar minimum. In general, the combined descending phase and solar minimum had comparatively more intense events than solar maximum and the ascending phases.

[41] One hypothesis to explain this is that during the descending and solar minima phases, polar and low-latitude equatorial coronal holes are larger and the HSSs emanating from them are more geoeffective. By the latter, we mean that the center of the HSSs where the speeds are ~ 750 to 800 km/s and the magnetic field variability $\Delta B/B_0$ is ~ 1 to 2 impinge on the magnetosphere (ΔB being the peak-to-peak amplitude of the transverse magnetic field). These solar wind features cause more intense and longer duration HILDCAA events.

3.8. Comparison of HILDCAA Characteristics Between Solar and Geomagnetic Minima

[42] The years 1986, 1996, and 2008 represent three consecutive solar activity minima with yearly mean $F_{10.7}$ values of ~ 74 , 72 , and 69 , respectively. We have considered the events occurring during solar minimum ± 1 year for comparative study (Table 3). Thus, since geomagnetic minimum typically occurs ~ 1 year after solar minimum [Echer *et al.*, 2011a; Tsurutani *et al.*, 2011b], these include geomagnetic minima as well. The numbers of HILDCAAs during the intervals were 13, 9, and 4, respectively. We intercompared possible differences in the characteristics of HILDCAAs among these solar minima, though it should be noted that the numbers of events are small for any statistical analysis. The events occurring during the recent minimum (2007–2009) were found to be appreciably weaker (AE_p $\sim 17\%$ and 14% lower) and short duration (D $\sim 35\%$ and 41% shorter) compared to the previous minima (1995–1997 and 1985–1987, respectively).

[43] This result is consistent with the overall lower geomagnetic activity around the recent solar minimum. For the 2008–2009 interval, the IMF Bz variances were examined by Tsurutani *et al.* [2011b] and Echer *et al.* [2011b] and it was shown that not only was the solar wind speed lower, but the IMF Bz variances were lower as well. Other possible causes behind the weak geomagnetic activity around the recent solar minimum are: (i) the low number of equatorial and low-latitude coronal holes, (ii) low IMF magnitudes, (iii) low solar wind speeds, (iv) weakness of magnetohydrodynamic forces in the solar wind, and (v) low energy transfer from solar wind to the magnetosphere during the period [de Toma, 2010, 2012; Tsurutani *et al.*, 2011b; Echer *et al.*, 2012].

4. Summary

[44] This paper presented, for the first time, the results of the statistical studies on the HILDCAAs using long-term (1975–2011) geomagnetic and solar wind/interplanetary databases. The results may be summarized as follows:

[45] 1. One hundred thirty-three AE events satisfying the “HILDCAA criteria” suggested by Tsurutani and Gonzalez [1987] have been identified from 1975 to 2011, a $3\frac{1}{2}$ solar cycle span (Figure 1). A list of events will be made available on request.

[46] 2. Of the 133 events, 99 had simultaneous interplanetary data available. Of these cases, 94% were associated with interplanetary HSSs. The remaining 6% of the cases occurred after the passage of ICMEs. The HSS-related HILDCAAs were typically associated with large-amplitude IMF Bz variances. The ICME-related events were characterized by small, steady southward Bz intervals or low-frequency fluctuations (Figures 2 and 3).

[47] 3. The solar cycle variation of HILDCAAs showed an occurrence peak ($\sim 6.8/\text{year}$) during the declining phase. An appreciable number of events were also observed during solar minimum ($\sim 3.5/\text{year}$). The occurrence frequencies were considerably lower in the ascending phase ($\sim 2.5/\text{year}$) and at solar maximum ($\sim 2.2/\text{year}$). Thus, HILDCAAs occurred during all four phases of the solar cycle, with those occurring during declining phases having an approximately three times greater probability than those in solar maximum and rising phase (Figure 5).

[48] 4. The HILDCAA events occurring during the descending phases were, on the average, $\sim 21\%$ longer in duration than those during the ascending phases. Similarly, the solar minimum events were $\sim 29\%$ longer than the solar maximum events. Also, the events during the descending phase and solar minimum were more intense than those during the ascending phase and solar maximum, respectively (Table 2).

[49] 5. The events occurring during the most recent solar minimum years (2007–2009) were found to be fewer in number, $\sim 17\%$, and 14% weaker in strength than those during previous solar minima of 1995–1997 and 1985–1987, respectively (Table 3). Also, the duration of the recent events were $\sim 35\%$ and 41% shorter than those of the two previous minima, respectively. Although the numbers of events during the intervals were small for any statistical analysis, the result is consistent with the overall lower geomagnetic activity around the recent solar minimum [de Toma, 2010, 2012; Echer *et al.*, 2011b, 2012; Tsurutani *et al.*, 2011b].

[50] 6. The peaks of the solar cycle variation of HILDCAAs were well correlated with the yearly average V_{sw} and number of days with HSSs ($V_{sw} \geq 500$ km/s) (Figures 7, 8). This result is consistent with item (4).

[51] 7. HILDCAA distributions did not exhibit any “classical” semiannual variations as observed for geomagnetic storms (Figure 6). During solar maximum, the number of events seemed to be larger during summer compared to equinoxes. The occurrences were consistently low during the month of November in all phases of the solar cycle. There were no seasonal dependences found. The results may suggest the effect of ionospheric ionization on the magnetic activities [Mursula et al., 2011].

5. Final Comments

[52] This study was done primarily to identify the solar cycle dependences of HILDCAA intervals and to form a database which could be used by investigators for the study of related phenomena. What was not covered in this paper is what HILDCAAs are from a physical viewpoint. This is clearly an important topic but beyond the scope of the present work. The justification for the name “HILDCAA” is given in Tsurutani et al. [2011a]. Notice that the word “substorm” is not included in this name (only AE activity), for good reason. Although there are substorms during HILDCAA intervals [Tsurutani et al., 2004], there is clearly much more happening in the magnetosphere/ionosphere system [Guarnieri, 2006; Guarnieri et al., 2006]. We encourage the interested reader to pursue this topic.

[53] The high IMF B_z variances and normalized variances during HILDCAA events most likely indicate interplanetary Alfvén waves that have been shown and discussed in many previous works [Tsurutani et al., 1982, 1990, 2011a, 2011b; Tsurutani and Gonzalez, 1987; Echer et al., 2011b]. They were not identified as such here because this was not the main focus of this paper. Based on the scenario presented by some of the present authors and many others mentioned in section 1, we predict that these HILDCAA intervals will be those characterized by intense outer zone chorus and enhanced relativistic electrons. We are interested in working with relativistic electron experimenters to determine if this prediction is correct or not.

[54] **Acknowledgments.** The work of RH is financially supported by Fundação de Amparo à Pesquisa do Estado de São Paulo (FAPESP) through post-doctoral research fellowship at INPE. One of the authors (EE) would like to thank the Brazilian CNPq (301233/2011-0) agency for financial support. Portions of this research were performed at the Jet Propulsion Laboratory, California Institute of Technology under contract with NASA. BTT wishes to thank P. Bellan for hosting him at the Applied Physics Department during his sabbatical stay at Caltech and M. Paetzold during his stay at the University of Cologne, Germany.

[55] Robert Lysak thanks the reviewers for their assistance in evaluating this paper.

References

- Akasofu, S.-I. (1981), Relationships between the AE and Dst indices during geomagnetic storms, *J. Geophys. Res.*, **86**, 4820–4822, doi:10.1029/JA086iA06p04820.
- Alves, M. V., E. Echer, and W. D. Gonzalez (2006) Geoeffectiveness of corotating interaction regions as measured by Dst index, *J. Geophys. Res.*, **111**, A07S05, doi:10.1029/2005JA011379.
- Baker, D. N., J. B. Blake, R. W. Klebesadel, and P. R. Higbie (1986), Highly relativistic electrons in the Earth’s outer magnetosphere: 1. Life-times and temporal history 1979–1984, *J. Geophys. Res.*, **91**, 4265–4276, doi:10.1029/JA091iA04p04265.
- Balogh, A., et al. (1999), The solar origin of corotating interaction regions and their formation in the inner heliosphere, *Space Sci. Rev.*, **89**, 141–178.
- Belcher, J. W., and L. Davis Jr., (1971), Large-amplitude Alfvén waves in the interplanetary medium: 2, *J. Geophys. Res.*, **76**, 3534–3563, doi:10.1029/JA076i016p03534.
- Borovsky, J. E., and J. T. Steinberg (2006), The “calm before the storm” in CIR/magnetosphere interactions: occurrence statistics, solar wind statistics and magnetospheric preconditioning, *J. Geophys. Res.*, **111**, A07S10, doi:10.1029/2005JA011397.
- Burlaga, L. F., E. Sittler, F. Mariani, and R. Schwenn (1981), Magnetic loop behind and interplanetary shock: Voyager, Helios and IMP-8 observations, *J. Geophys. Res.*, **86**, 6673–6684, doi:10.1029/JA086iA08p06673.
- Burtis, W. J., and R. A. Helliwell (1969), Banded chorus – A new type of VLF radiation observed in the magnetosphere by OGO-I and OGO-3, *J. Geophys. Res.*, **74**, 3002–3010.
- Chakraborty, S. K., and R. Hajra (2010), Variability of total electron content near the crest of the equatorial anomaly during moderate geomagnetic storms, *J. Atmos. Sol. Terr. Phys.*, **72**, 900–911.
- Clua de Gonzalez, A. L., W. D. Gonzalez, S. L. G. Dutra, and B. T. Tsurutani (1993), Periodic variation in the geomagnetic activity: A study based on the Ap index, *J. Geophys. Res.*, **98**, 9215–9231, doi:10.1029/92JA02200.
- Davis, T. N., and M. Sugiura (1966), Auroral electrojet activity index AE and its universal time variations, *J. Geophys. Res.*, **71**, 785–801, doi:10.1029/JZ071i003p00785.
- de Toma, G. (2010), Evolution of coronal holes and implications for high-speed solar wind during the minimum between cycles 23 and 24, *Solar Phys.*, doi:10.1007/s11207-010-9677-2.
- de Toma, G. (2012), Polar magnetic fields and coronal holes during the recent solar minima, *Proc. Int. Astron. Union*, **286**, 101–112, doi:10.1017/S1743921312004711.
- Doherty, P. H., J. A. Klobuchar, and J. M. Kunches (2000), Eye on the ionosphere: the correlation between solar 10.7 cm radio flux and ionospheric range delay, *GPS sol.*, **3**, 75–79.
- Dungey, J. W. (1961), Interplanetary magnetic field and the auroral zones, *Phys. Rev. Lett.*, **6**, 47–48.
- Echer, E., W. D. Gonzalez, and B. T. Tsurutani (2008), Interplanetary conditions leading to superintense geomagnetic storms ($Dst \leq -250$ nT) during solar cycle 23, *Geophys. Res. Lett.*, **35**, L06S03, doi:10.1029/2007GL031755.
- Echer, E., W. D. Gonzalez, and B. T. Tsurutani (2011a), Statistical studies of geomagnetic storms with peak $Dst \leq -50$ nT from 1957 to 2008, *J. Atmos. Sol. Terr. Phys.*, **73**, 1454–1459.
- Echer, E., B. T. Tsurutani, W. D. Gonzalez, and J. U. Kozyra (2011b), High speed stream properties and related geomagnetic activity during the whole heliosphere interval (WHI): 20 March to April 2008, *Solar Phys.*, doi:10.1007/s11207-011-9739-0.
- Echer, E., B. T. Tsurutani, and W. D. Gonzalez (2012), Extremely low geomagnetic activity during the recent deep solar cycle minimum, *Proc. Int. Astron. Union*, **7**, 200–209, doi:10.1017/S174392131200484X.
- Echer, E., B. T. Tsurutani, and W. D. Gonzalez (2013), Interplanetary origins of moderate (-100 nT $< Dst \leq -50$ nT) geomagnetic storms during solar cycle 23 (1996–2008), *J. Geophys. Res. Space Physics*, **118**, 385–392, doi:10.1029/2012JA018086.
- Gonzalez, W. D., and F. S. Mozer (1974), A quantitative model for the potential resulting from reconnection with an arbitrary interplanetary magnetic field, *J. Geophys. Res.*, **79**, 4186–4194, doi:10.1029/JA079i028p04186.
- Gonzalez, W. D., A. L. C. Gonzalez, and B. T. Tsurutani (1990), Dual-peak solar cycle distribution of intense geomagnetic storms, *Planet. Space Sci.*, **38**, 181–187.
- Gonzalez, W. D., J. A. Joselyn, Y. Kamide, H. W. Kroehl, G. Rostoker, B. T. Tsurutani, and V. Vasyliunas (1994), What is a geomagnetic storm?, *J. Geophys. Res.*, **99**, 5771–5792.
- Gonzalez, W. D., B. T. Tsurutani, and A. L. Clua de Gonzalez (1999), Interplanetary origin of geomagnetic storms, *Space Sci. Rev.*, **88**, 529–562.
- Gonzalez, W. D., F. L. Guarnieri, A. L. Clua-Gonzalez, E. Echer, M. V. Alves, T. Oginoo, and B. T. Tsurutani (2006), Magnetospheric energetics during HILDCAAs, in *Recurrent Magnetic Storms: Corotating Solar Wind Streams*, Geophys. Monogr. Ser., vol. 167, edited by B. Tsurutani et al., pp. 175–182, AGU, Washington, D.C., doi:10.1029/167GM15.
- Gonzalez, W. D., E. Echer, A. L. Clua de Gonzalez, and B. T. Tsurutani (2007), Interplanetary origin of intense geomagnetic storms ($Dst < -100$ nT) during solar cycle 23, *Geophys. Res. Lett.*, **34**, L06101, doi:10.1029/2006GL028879.
- Gopalswamy, N., S. Nunes, S. Yashiro, and R. A. Howard (2004), Variability of solar eruptions during cycle 23, *Adv. Space Res.*, **34**, 391–396.

- Gosling, J. T., S. J. Bame, D. J. McComas, and J. L. Phillips (1990), Coronal mass ejections and large geomagnetic storms, *Geophys. Res. Lett.*, **17**, 901–904, doi:10.1029/GL017i007p00901.
- Guarnieri, F. L. (2006), The nature of auroras during high-intensity long-duration continuous AE activity (HILDCAA) events: 1998–2001, in *Recurrent Magnetic Storms: Corotating Solar Wind Streams*, Geophys. Monogr. Ser., vol. 167, edited by B. T. Tsurutani et al., pp. 235–243, AGU, Washington, D.C.
- Guarnieri, F. L., B. T. Tsurutani, W. D. Gonzalez, E. Echer, A. L. C. Gonzalez, M. Grande, and F. Soraas (2006), ICME and CIR storms with particular emphasis on HILDCAA events, *ILWS Workshop 2006*, Goa.
- Gurnett, D. A., and B. J. O'Brien (1964), High-latitude geophysical studies with satellite Injun 3: 5. Very-low-frequency electromagnetic radiation, *J. Geophys. Res.*, **69**, 65–89.
- Hajra, R. (2011), A study on the variability of total electron content near the crest of the equatorial anomaly in the Indian zone, PhD thesis, University of Calcutta, India.
- Horne, R. B., and R. M. Thorne (1998), Potential waves for relativistic electron scattering and stochastic acceleration during magnetic storms, *Geophys. Res. Lett.*, **25**, 3011–3014, doi:10.1029/98GL01002.
- Hundhausen, A. J. (1973), Nonlinear model of high-speed solar wind streams, *J. Geophys. Res.*, **78**, 1528–1542, doi:10.1029/JA078i010p01528.
- Inan, U. S., T. F. Bell, and R. A. Helliwell (1978), Nonlinear pitch angle scattering of energetic electrons by coherent VLF waves in the magnetosphere, *J. Geophys. Res.*, **83**, 3235–3253.
- Kennel, C. F., and H. E. Petschek (1966), Limit on stably trapped particle fluxes, *J. Geophys. Res.*, **71**, 1–28, doi:10.1029/JZ071i001p00001.
- Klein, L. W., and L. F. Burlaga (1982), Interplanetary magnetic clouds At 1 AU, *J. Geophys. Res.*, **87**, 613–624, doi:10.1029/JA087iA02p00613.
- Kozyra, J. U., et al. (2006), Response of the upper/middle atmosphere to coronal holes and powerful high-speed solar wind streams in 2003, in *Recurrent Magnetic Storms: Corotating Solar Wind Streams*, Geophys. Monogr. Ser., vol. 167, edited by B. T. Tsurutani et al., p. 319, AGU, Washington, D.C.
- Krieger, A. S., A. F. Timothy, and E. C. Roelof (1973), A coronal hole and its identification as the source of a high velocity solar wind stream, *Solar Phys.*, **29**, 505–525.
- Lakhina, G. S., B. T. Tsurutani, O. P. Verkhoglyadova, and J. S. Pickett (2010), Pitch angle transport of electrons due to cyclotron interactions with the coherent chorus subelements, *J. Geophys. Res.*, **115**, A00F15, doi:10.1029/2009JA014885.
- Li, X., D. N. Baker, M. A. Temerin, T. E. Cayton, E. G. D. Reeves, R. A. Christensen, J. B. Blake, M. D. Looper, R. Nakamura, and S. G. Kanekal (1997), Multi-satellite observations of the outer zone electron variation during the November 3–4, 1993, magnetic storm, *J. Geophys. Res.*, **102**, 14,123–14,140.
- Lopez, R. E., and J. W. Freeman (1986), Solar wind proton temperature-velocity relationship, *J. Geophys. Res.*, **91**, 1701–1705.
- Lorentzen, K. R., J. B. Blake, U. S. Inan, and J. Bortnik (2001), Observations of relativistic electron microbursts in association with VLF chorus, *J. Geophys. Res.*, **106**, 6017–6027, doi:10.1029/2000JA003018.
- Meredith, N. P., M. Cain, R. B. Horne, R. M. Thorne, D. Summers, and R. R. Anderson (2003), Evidence for chorus-driven electron acceleration to relativistic energies from a survey of geomagnetically disturbed periods, *J. Geophys. Res.*, **108**(A6), 1248, doi:10.1029/2002JA009764.
- Mursula, K., E. Tanskanen, and J. J. Love (2011), Spring-fall asymmetry of substorm strength, geomagnetic activity and solar wind: implications for semiannual variation and solar hemispheric asymmetry, *Geophys. Res. Lett.*, **38**, L06104, doi:10.1029/2011GL046751.
- Nakamura, R., M. Isowa, Y. Kamide, D. N. Baker, J. B. Blake, and M. Looper (2000), SAMPEX observations of precipitation bursts in the outer radiation belt, *J. Geophys. Res.*, **105**, 15,875–15,885, doi:10.1029/2000JA900018.
- Obara, T., T. Nagatsuma, M. Den, E. Sagawa, and T. G. Onsager (2000), Effects of the IMF and substorms on the rapid enhancement of relativistic electrons in the outer radiation belt during storm recovery phase, *Adv. Space Res.*, **26**, 89–92, doi:10.1016/S0273-1177(99)01030-3.
- Obridko, V. N., E. V. Ivanov, A. Özgüç, A. Kilcik, and V. B. Yurchyshyn (2012), Coronal mass ejections and the index of effective solar multipole, *Sol. Phys.*, **281**, 779–792, doi:10.1007/s11207-012-0096-4.
- Omura, Y., Y. Katoh, and D. Summers (2008), Theory and simulation of the generation of whistler-mode chorus, *J. Geophys. Res.*, **113**, A04223, doi:10.1029/2007JA012622.
- Paulikas, G., and J. B. Blake (1979), Effects of the solar wind on magnetospheric dynamics: Energetic electrons at the synchronous orbit, in *Quantitative Modeling of Magnetospheric Processes*, Geophys. Monogr. Ser., vol. 21, edited by W. Olsen, p. 21, AGU, Washington, D.C.
- Pizzo, V. J. (1985), Interplanetary shocks on the large scale: a retrospective on the last decade's theoretical efforts, in *Collisionless Shocks in the Heliosphere: Reviews of Current Research*, Geophys. Monogr. Ser., **35**, edited by B. T. Tsurutani and R. G. Stone, 51–68, AGU, Washington, D.C., doi:10.1029/GM035p0051.
- Richardson, I. G., H. V. Cane, and E. W. Cliver (2002), Sources of geomagnetic activity during nearly three solar cycles (1972–2000), *J. Geophys. Res.*, **107**(A8), A81187, doi:10.1029/2001JA000504.
- Rostoker, G. (1972), Geomagnetic indices, *Rev. Geophys.*, **10**, 935–950, doi:10.1029/RG010i004p00935.
- Sheeley, N. R., Jr., J. W. Harvey, and W. C. Feldman (1976), Coronal holes, solar wind streams and recurrent geomagnetic disturbances: 1973–1976, *Sol. Phys.*, **49**, 271–278.
- Smith, E. J., and J. H. Wolfe (1976), Observations of interaction regions and corotating shocks between one and five AU: Pioneers 10 and 11, *Geophys. Res. Lett.*, **3**, 137–140, doi:10.1029/GL003i003p00137.
- Smith, E. J., B. T. Tsurutani, and R. L. Rosenberg (1978), Observations of the interplanetary sector structure up to heliographic latitudes of 16°: Pioneer 11, *J. Geophys. Res.*, **83**, 717–724.
- Sugiura, M. (1964), *Hourly Values of Equatorial Dst for the IGY*, Annual International Geophysical Year, vol. 35, p. 9, Pergamon, New York.
- Summers, D., R. M. Thorne, and F. Xiao (1998), Relativistic theory of wave-particle resonant diffusion with application to electron acceleration in the magnetosphere, *J. Geophys. Res.*, **103**, 20,487–20,500, doi:10.1029/98JA01740.
- Summers, D., B. Ni, and N. P. Meredith (2007), Timescales for radiation belt electron acceleration and loss due to resonant wave-particle interactions: 2. Evaluation for VLF chorus, ELF hiss, and electromagnetic ion cyclotron waves, *J. Geophys. Res.*, **112**, A04207, doi:10.1029/2006JA011993.
- Thorne, R. M., T. P. O'Brien, Y. Y. Shprits, D. Summers, and R. B. Horne (2005), Timescale for MeV electron microburst loss during geomagnetic storms, *J. Geophys. Res.*, **110**, A09202, doi:10.1029/2004JA010882.
- Tsurutani, B. T., and W. D. Gonzalez (1987), The cause of high-intensity long-duration continuous AE activity (HILDCAAs): interplanetary Alfvén wave trains, *Planet. Space Sci.*, **35**, 405–412.
- Tsurutani, B. T., and W. D. Gonzalez (1997), The interplanetary causes of magnetic storms: a review, in *Magnetic Storms*, Geophys. Monogr. Ser., vol. 98, edited by B. T. Tsurutani et al., pp. 77–89, AGU, Washington, D.C.
- Tsurutani, B. T., and G. S. Lakhina (1997), Some basic concepts of wave-particle interactions in collisionless plasmas, *Rev. Geophys.*, **35**, 491–501, doi:10.1029/97RG02200.
- Tsurutani, B. T., and E. J. Smith (1974), Postmidnight chorus: A substorm phenomenon, *J. Geophys. Res.*, **79**, 118–127, doi:10.1029/JA079i001p00118.
- Tsurutani, B. T., and E. J. Smith (1977), Two types of magnetospheric ELF chorus and their substorm dependences, *J. Geophys. Res.*, **82**, 5112–5128, doi:10.1029/JA082i032p05112.
- Tsurutani, B. T., E. J. Smith, H. I. West, and R. M. Buck (1979), Chorus, energetic electrons and magnetospheric substorms, in *Waves Instabilities in Space Plasmas*, edited by P. J. Palmadesso and K. Papadopoulos, p. 55, D. Reidel, Norwell, Mass.
- Tsurutani, B. T., E. J. Smith, R. R. Anderson, K. W. Ogilvie, J. D. Scudder, D. N. Baker, and S. J. Bame (1982), Lion roars and nonoscillatory drift mirror waves in the magnetosheath, *J. Geophys. Res.*, **87**, 6060–6072, doi:10.1029/JA087iA08p06060.
- Tsurutani, B. T., W. D. Gonzalez, F. Tang, S. I. Akasofu, and E. J. Smith (1988), Origin of interplanetary southward magnetic fields responsible for major magnetic storms near solar maximum (1978–1979), *J. Geophys. Res.*, **93**, 8519–8531, doi:10.1029/JA093iA08p08519.
- Tsurutani, B. T., T. Gould, B. E. Goldstein, W. D. Gonzalez, and M. Sugiura (1990), Interplanetary Alfvén waves and auroral (substorm) activity: IMP 8, *J. Geophys. Res.*, **95**, 2241–2252, doi:10.1029/JA095iA03p02241.
- Tsurutani, B. T., W. D. Gonzalez, F. Tang, and Y. T. Lee (1992), Great magnetic storms, *Geophys. Res. Lett.*, **19**, 73–76.
- Tsurutani, B. T., W. D. Gonzalez, A. L. C. Gonzalez, F. Tang, J. K. Arballo, and M. Okada (1995), Interplanetary origin of geomagnetic activity in the declining phase of the solar cycle, *J. Geophys. Res.*, **100**, 21,717–21,733, doi:10.1029/95JA01476.
- Tsurutani, B. T., W. D. Gonzalez, F. Guarnieri, Y. Kamide, X. Zhou, and J. K. Arballo (2004), Are high-intensity long-duration continuous AE activity (HILDCAA) events substorm expansion events?, *J. Atmos. Sol. Terr. Phys.*, **66**, 167–176.
- Tsurutani, B. T., G. S. Lakhina, J. S. Pickett, F. L. Guarnieri, N. Lin, and B. E. Goldstein (2005), Nonlinear Alfvén waves, discontinuities, proton perpendicular acceleration, and magnetic holes/decreases in interplanetary space and the magnetosphere: intermediate shocks?, *Nonlinear Proc. Geophys.*, **12**, 321–336.
- Tsurutani, B. T., et al. (2006a), Corotating solar wind streams and recurrent geomagnetic activity: A review, *J. Geophys. Res.*, **111**, A07S01, doi:10.1029/2005JA011273.

- Tsurutani, B. T., R. L. McPherron, W. D. Gonzalez, G. Lu, N. Gopalswamy, and F. L. Guarnieri (2006b), Magnetic storms caused by corotating solar wind streams, in *Recurrent Magnetic Storms: Corotating Solar Wind Streams*, Geophys. Monogr. Ser., vol. 167, edited by B. T. Tsurutani et al., pp. 1–17, AGU, Washington, D.C.
- Tsurutani, B. T., O. P. Verkhoglyadova, G. S. Lakhina, and S. Yagitani (2009), Properties of dayside outer zone chorus during HILDCAA events: Loss of energetic electrons, *J. Geophys. Res.*, *114*, A03207, doi:10.1029/2008JA013353.
- Tsurutani, B. T., E. Echer, F. L. Guarnieri, and W. D. Gonzalez (2011a), The properties of two solar wind high speed streams and related geomagnetic activity during the declining phase of solar cycle 23, *J. Atmos. Sol. Terr. Phys.*, *73*, 164–177.
- Tsurutani, B. T., E. Echer, and W. D. Gonzalez (2011b), The solar and interplanetary causes of the recent minimum in geomagnetic activity (MGA23): A combination of midlatitude small coronal holes, low IMF Bz variances, low solar wind speeds and low solar magnetic fields, *Ann. Geophys.*, *29*, 839–849.
- Tsurutani, B. T., G. S. Lakhina, and O. P. Verkhoglyadova (2013), Energetic electron (>10 keV) microburst precipitation, ~5–15 s X-ray pulsations, chorus, and wave-particle interactions: A review, *J. Geophys. Res. Space Physics*, *118*, 2296–2312, doi:10.1002/jgra.50264.
- Turner, N. E., E. J. Mitchell, D. J. Knipp, and B. A. Emery (2006), Energetics of magnetic storms driven by corotating interaction regions: a study of geoeffectiveness, in *Recurrent Magnetic Storms: Corotating Solar Wind Streams*, Geophys. Monogr. Ser., vol. 167, edited by B. T. Tsurutani et al., pp. 113–124, AGU, Washington, D.C.
- Webb, D. F., and R. A. Howard (1994), The solar cycle variation of coronal mass ejections and the solar wind mass flux, *J. Geophys. Res.*, *99*, 4201–4220, doi:10.1029/93JA02742.
- Winterhalter, D., E. J. Smith, M. E. Burton, N. Murphy, and D. J. McComas (1994), The heliospheric plasma sheet, *J. Geophys. Res.*, *99*, 6667–6680.